Measurement comparison of goniometric scatterometry and coherent Fourier scatterometry

J. Endres, N. Kumar*, P. Petrik*, M.-A. Henn, S. Heidenreich, S. F. Pereira, H. P. Urbach, B. Bodermann,

Physikalisch-Technische Bundesanstalt (PTB), Bundesallee 100, 38116 Braunschweig, Germany

* Technische Univ. Delft, Van der Waalsweg 8, 2628CH Delft, The Netherlands

ABSTRACT

Scatterometry is a common tool for the dimensional characterization of periodic nanostructures. In this paper we compare measurement results of two different scatterometric methods: a goniometric DUV scatterometer and a coherent scanning Fourier scatterometer.

We present a comparison between these two methods by analyzing the measurement results on a silicon wafer with 1D gratings having periods between 300 nm and 600 nm. The measurements have been performed with PTB's goniometric DUV scatterometer and the coherent scanning Fourier scatterometer at TU Delft. Moreover for the parameter reconstruction of the goniometric measurement data, we apply a maximum likelihood estimation, which provides the statistical error model parameters directly from measurement data.

Keywords: Scatterometry, CD, pitch, inverse diffraction problem

1. INTRODUCTION

Scatterometry is a standard metrology tool for the dimensional and optical characterization of periodic micro- and nanostructured surfaces in industry. The geometric profile of the underlying structure is reconstructed from the measured scatterograms by applying inverse rigorous calculations. From the theoretical viewpoint one has to solve an inverse problem which is in general improperly-posed. However, with additional a-priori information, e.g. by specifying the structure as a certain type of grating, which can be described by a finite number of parameters, it is possible to find a best-fit solution for the structure profile [1].

Compared with other well established measurement techniques like atomic force microscopy (AFM) and scanning electron microscopy (SEM), scatterometry as a non-imaging optical metrology is fast, non-destructive, highly repeatable and not diffraction limited. It is in-situ capable and can be easily integrated in existing production lines.

Over time, various scatterometric methods have been proposed and implemented which mainly differ from each other by utilizing different properties of the diffracted light: diffraction angle, wavelength, phase and intensity or polarization state. The resulting measurement techniques are classified in goniometric, reflectometric, spectrocscopic or ellipsometric systems. Moreover, by using a microscopic setup and imaging the Fourier plane of the objective lens one can record the complete 3D diffraction pattern. The technique is called Fourier scatterometry and has recently been considerably improved and extended [2-5].

Especially spectroscopic scatterometry methods have evolved as standard procedures in semiconductor industry for photomask and wafer inspection. They are used for the characterization of the edge profiles and the critical dimensions (CD) of the etched structures, but also for evaluating other important process parameters such as diffraction based overlay (DBO). By applying library based methodologies for the CD profile extraction they are in-situ capable [6]. Typically a discharge lamp is used for the illumination in spectroscopic systems providing spatially incoherent light. Recently, it has been shown that using a spatially coherent light source in a Fourier scatterometer can significantly increase the sensitivity with respect to the geometric parameters of the sample under test. The technique is also called coherent Fourier scatterometry (CFS) [7].

In scanning coherent Fourier scatterometry, the illumination spot of a spatially coherent laser source is scanned over the sample within one period of the grating. This method extends the conventional CFS by using the principle of temporal phase-shifting interferometry. It has been shown that under certain conditions the improvement in sensitivity is more

Optical Micro- and Nanometrology V, edited by Christophe Gorecki, Anand Krishna Asundi,
Wolfgang Osten, Proc. of SPIE Vol. 9132, 913208 · © 2014 SPIE
CCC code: 0277-786X/14/$18 · doi: 10.1117/12.2052819

Downloaded From: http://www.spiedl.org/ on 01/16/2015 Terms of Use: http://spiedl.org/terms

than fourfold compared to incoherent optical scatterometry [7, 8]. In this paper we show measurements done with a scanning Fourier scatterometer on a silicon 1D line grating with 600 nm pitch and present the reconstruction results for the grating parameters.

Moreover, the results are compared with the measurements performed by a goniometric DUV scatterometer where the light intensity and polarization state of the diffracted optical far field are measured at different angels of incidence (AOI). The typically high angular resolution and high dynamic range together with a wide scope of AOI's provide sufficient information for the reconstruction of the structure parameters under the condition that enough diffraction orders are available.

The paper is organized as follows: In section 2, we give a short description of the applied measurement methods and the corresponding experimental setup. Section 3 concentrates on the parameter reconstruction and the statistical methods used for the uncertainty estimation. The measurement results are presented in section 4 and section 5 contains the conclusion.

2. MEASUREMENT CONFIGURATION

The measurements have been performed with two different scatterometric measurement systems: a goniometric DUV scatterometer at PTB [9, 10] and a coherent scanning Fourier scatterometer at TU Delft [4, 8].

Goniometric DUV scatterometry

The goniometric DUV scatterometer records the scattering angle and the diffraction efficiencies for the optical far fields for different angles of incidence (AOI). Both for the illumination and the detection an arbitrary linear polarization state can be chosen.

Figure 1 shows a schematic illustration of the experimental setup. For the illumination both a pulsed 193 nm DUV laser and a 266 nm CW laser can be coupled into the beam path of the system by means of a switchable mirror. Next, a Dove prism divides the beam into a signal and a reference part with a constant ratio which allows to compensate for power fluctuations of the laser source. The signal beam is further prepared with a set of polarization optics and finally focused onto the sample with the aid of a telescope providing a spot size between 40 µm and 4 mm. The light diffracted from the sample is collected at the entrance of the detector, analyzed with respect to its polarization state and finally guided to the signal detector.

The high dynamic range and detection linearity with more than 7 orders of magnitude together with the high angular resolution and long-time stability lead to high sensitivity and repeatable measurements of the diffraction patterns.

The diffraction efficiencies are obtained by integrating the intensity profile of the diffracted peaks normalized to the intensity of the incoming beam without sample. The uncertainties are determined from the correlation between the incident and the diffracted beam profile.

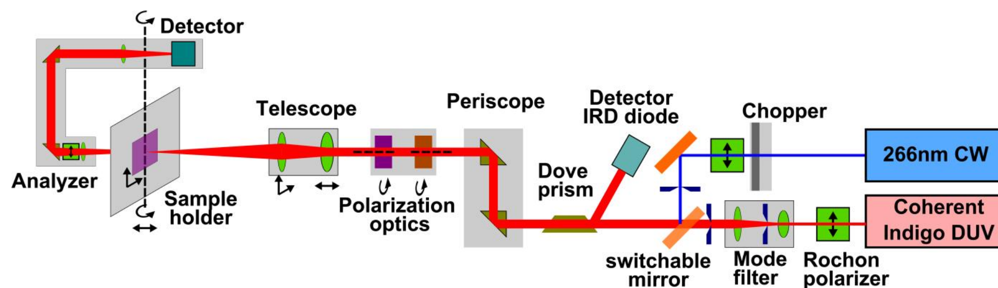

Figure 1 Schematic experimental setup of PTB's DUV scatterometer.

The measurements on the sample under test were realized for AOIs in the range between -85° and 85° at five different sample positions. The illumination wavelength was set at 266 nm. Each measurement has been done with s- and p-polarized light. The diameter of the incident beam at the sample positions was 40 µm.

Downloaded From: http://www.spiedl.org/ on 01/16/2015 Terms of Use: http://spiedl.org/terms

Coherent scanning Fourier scatterometry

Fourier scatterometry provides a means of measuring scattered light over a large range of incident and detection angles. The light is focused on the sample, whereas the angle-dependent response is collected using the same lens. In the back focal plane of the lens, each point uniquely corresponds to a certain scattered direction. This way, by imaging the back focal plane, the angular spectrum of the reflection and diffraction can be recorded. Using high numerical aperture (NA) lenses, the range of incident and reflected angles can be as large as -64° to 64° using e.g. of a lens of NA = 0.9 with azimuth angles between 0° and 360°. The sensitivity can be increased by extending the instrumentations utilizing phase information by applying a scanning focused spot [7, 8], by interferometry or by adding polarization information using ellipsometry [11, 12].

The measurement setup is shown in figure 2. The light from a HeNe laser working at a wavelength of 632.8 nm is focused using lens L1 and coupled to a single mode fiber (SMF). It is then split into two other single-mode fibers using a fiber coupler (FC). The output of these two fibers is collimated by lenses L2 and L3. The beam passing lens L2 is focused by a microscope objective (MO) onto the grating. Numerical apertures of NA = 0.4 and NA = 0.9 can be used in our experiments corresponding to spot radii of $r = 0.61\lambda/NA$ of 965 nm and 429 nm, respectively. The measurements described in this publication have all been performed using the larger NA.

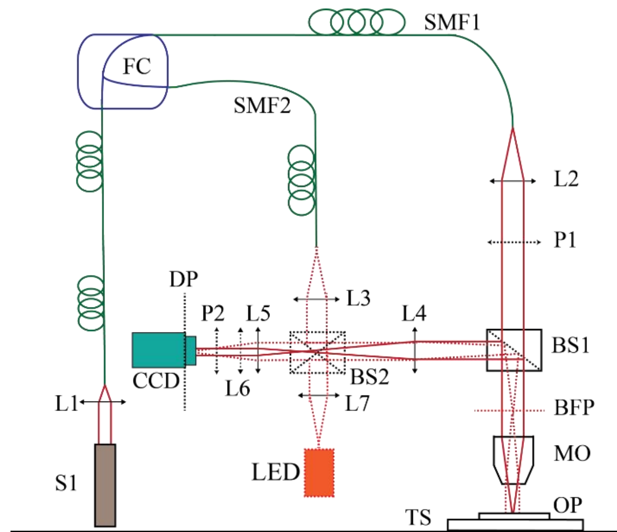

Figure 2 Experimental setup of a Fourier scatterometer with a fiber coupler (FC), beam splitters (BS), polarizers (P), and lenses for coupling (L1), collimating (L2, L3, L7) and imaging (L4, L5 and L6). Lenses L4 and L5 form a telescopic system with focal lengths of 250 mm and 100 mm, respectively. BFP denotes the back focal plane of the microscope objective (MO). The laser (S1) is a HeNe type working at a wavelength of 632.8 nm. The LED source has a wavelength of 670 nm. The beam paths for measurement and alignment are denoted by solid and dashed red lines, respectively. The dashed beams are blocked and the dashed lens L6 is removed for the measurements; the analyser P2 is used as required.

The light diffracted from the sample is collected by the same MO (epi-illumination), the back focal plane (BFP) of which is imaged by lenses L4 and L5 onto the CCD camera. The magnification has been adjusted by using proper lenses for L4 and L5 to match the size of the BFP to the size of the CCD (1600x1200 pixels, pixel size of 3.8 μm). The light collimated by L3 is used for the alignment of lens L4. The LED source (λ=670 nm) with lenses L6 and L7 serves for imaging the grating target to monitor the position of the focused spot. The sample can be moved within the object plane (OP) by means of a translation stage (TS).

3. PARAMETER RECONSTRUCTION

For the parameter reconstruction one has to define a geometric model and then to combine rigorous forward simulations with a nonlinear optimization procedure to obtain the best fit solution of the structure parameters of the model.

Downloaded From: http://www.spiedl.org/ on 01/16/2015 Terms of Use: http://spiedl.org/terms

Geometric model

To solve the inverse problem and reconstruct the structure profile, a certain amount of a-priori knowledge is required. The real grating structure placed on top of the silicon substrate is approximated by a simple trapezoidal model. Both the substrate as well as the structures may be covered by an oxide layer on top. Thus the model comprises the following set of structure parameters: middle CD, side wall angle *SWA*, structure height h and oxide layer thickness L. The layout of the model and the definition of the geometric parameters are given in figure 3.

The geometric model used for the Fourier scatterometric simulations has been slightly simplified by neglecting an oxide layer at the side walls of the grating profile for reasons of limited computational resources. Moreover the simulation of the scatterograms requires an additional free parameter: the bias value describes the shift of the focused spot position regarding to the grating lines.

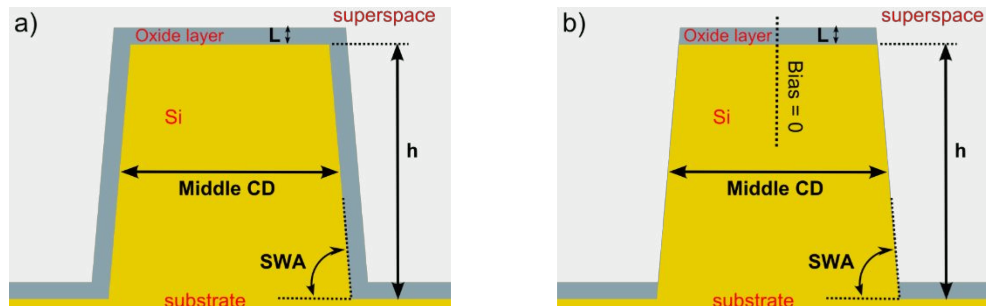

Figure 3 Geometric models with reconstruction parameters indicated. The model comprise the Si substrate with oxide layer on top. a) Model as applied for the DUV scatterometry measurements b) Model as applied for the Fourier scatterometry: the oxide layer at the side walls of the profile is omitted.

The substrate is assumed to be (100)-orientated crystalline Si. The refractive index of Si is taken form literature whereas the refractive index of the oxide layer is determined from reflection measurements as well as from ellipsometric measurements on the substrate in unstructured areas. Table 1 shows the final values used for the rigorous simulations.

Layer	DUV scatterometer @ 266 nm	Fourier scatterometer @ 632.8 nm
Si	2.10+4.41j	3.87+0.0158j
Oxide	1.81	1.46

Table 1 Refractive indices of the layer system for the rigorous simulation.

Rigorous simulations

The forward computations to solve the Helmholtz equation for a given set of grating parameters have been performed by two different methods: for practical reasons for the simulation of the Fourier scatterometric data the rigorous coupled wave analysis (RCWA) [14] has been used whereas the efficiencies for the goniometric setup are calculated by the finite element method (FEM) [15].

It has been verified that the simulation results from the RCWA-based and FEM-based Maxwell solvers agree if the solver specific accuracy parameters like mesh discretisation, polynomial order of the Ansatz functions for FEM and the number of spatial harmonics for RCWA are set correctly.

For the used RCWA implementation it is difficult to model edge corner rounding so that we neglected corner rounding effects for the sake of comparability between the RCWA and the FEM model although results in [10] propose an improvement of the fit results if corner rounding is included.

Best fit solution and measurement uncertainty

The reconstruction parameters are found as best fit solution between measurement data and rigorously calculated data by means of a nonlinear optimization procedure. The evaluation of the Fourier scatterometric data follows a standard

Downloaded From: http://www.spiedl.org/ on 01/16/2015 Terms of Use: http://spiedl.org/terms

nonlinear optimization scheme combining global and gradient based local solvers. The sensitivity with respect to the middle CD value and the structure height are approximately 2-3 nm, and for the SWA 5°.

The goniometric scatterometry data has been evaluated with two different methods: a nonlinear least squares optimization routine and a more advanced optimization method based on the maximum likelihood estimation (MLE). For the least squares optimisation a combination of a global optimisation strategy applying a differential evolution algorithm and a local optimisation using standard gradient based methods is applied to ensure, that the global minimum is found. In the comparison with conventional least squares methods, the MLE allows for an even more consistent reconstructions and prevents better from systematic errors when applied to scatterometry [1, 16]. Uncertainties are determined by the Fisher information matrix. Here, the covariance matrix of the likelihood is approximated by the inverse of the negative second derivative of the logarithm of the likelihood function. Furthermore, line roughness could be and has be taken into account. Line roughness is damping the diffraction efficiencies by a Debye-Waller like factor and affects the accuracy of reconstruction results by systematic errors [17, 18]. Recently, this effect was discussed for goniometric DUV scatterometry [19]. Here we present and compare optimisation results using both methods. The MLE analysis however, is preliminary in the sense, that for efficiency reasons only a reduced set of the measured data (for angles of incidence < 49°) has been used.

4. MEASUREMENT RESULTS

Sample under test

The measurements were performed on an etched silicon 1D-line grating fabricated by Eulitha AG (Villigen, Switzerland). The measurement field has overall dimensions of 10 mm x 10 mm. The geometrical dimensions for the 1D line structure as quoted by the manufacturer are: 301 nm middle CD, 600 nm pitch and 345 nm etch depth. Moreover, the substrate should consist of crystalline silicon in (100)-orientation with a native oxide layer of typically 2 nm thickness on top. However, both $\Theta - 2\Theta$ reflectance measurements with the DUV scatterometer and ellipsometric measurements within the unstructured area of the wafer imply to have a surface layer with thickness between 4 nm and 7 nm. Although one cannot confirm a pure native or thermal oxide layer, in a first approximation it can be modelled as a simple oxide layer with effective refractive index. The oxide layer thickness was included as free parameter in the reconstruction since one cannot expect to have a uniform layer thickness on both the substrate and the structured area, as mentioned above.

Reconstruction results

The measurement data and the best fit solution for each scatterometric system are shown in figures 4 and 5. The experimental and simulated far field intensities obtained with the Fourier scatterometer as well as their differences are plotted in figure 4 for both parallel (TE) and perpendicular (TM) polarizations referred to the grating lines. In both cases one can clearly identify the areas where the 0th and 1st orders are overlapping. The simulations are in good agreement with the measurement data. The minor differences can be ascribed to both measurement noise and imperfections in modelling aberrations.

The measured diffraction efficiencies for the DUV scatterometer are shown in figure 5, but for reasons of clarity only one data set (p-polarized illumination, sample position 1) is depicted. The best fit solution of the least squares fit reproduces the shape and the features of the measurement data and agrees also quantitatively well for the (larger) zero, ± first and ± third diffraction order. For the higher (and weaker) ± second and ± fourth diffraction orders measurement and simulation differ significantly, which may be an indication for using a too basic geometric model as stated in [10]. In addition we observed relative variations of the diffraction efficiencies within several percent for measurements at different sample positions. This may be caused by sample in homogeneities or surface roughness and will affect the reconstruction result, too.

Downloaded From: http://www.spiedl.org/ on 01/16/2015 Terms of Use: http://spiedl.org/terms

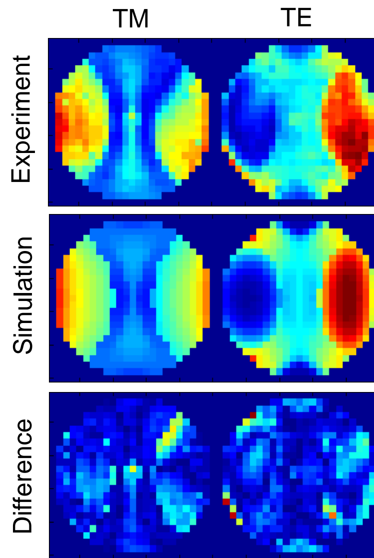

Figure 4 Far field intensities measured by coherent Fourier scatterometry together with the best fit solution and the corresponding residuals. The color scale is normalized with linear mapping between blue=low intensity and red=high intensity.

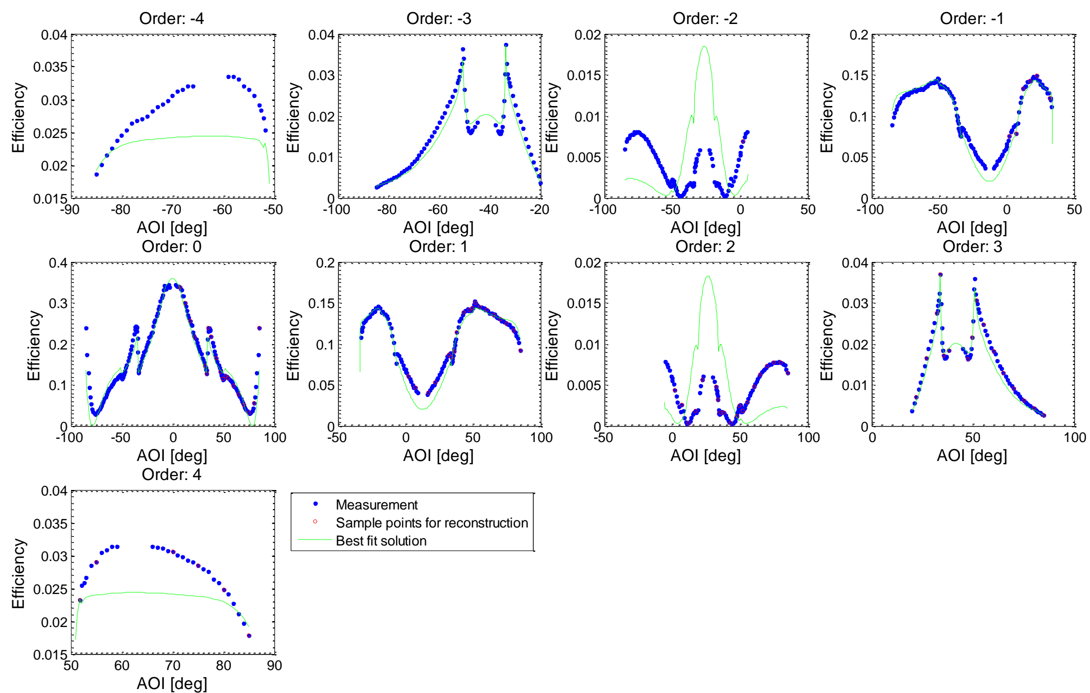

Figure 5 Diffraction efficiencies measured by DUV scatterometry together with the least squares fit solution for all observed diffraction orders. The sample points used for the reconstruction are marked red. Only one exemplary data set for p-polarized illumination at position 1 is shown.

Downloaded From: http://www.spiedl.org/ on 01/16/2015 Terms of Use: http://spiedl.org/terms

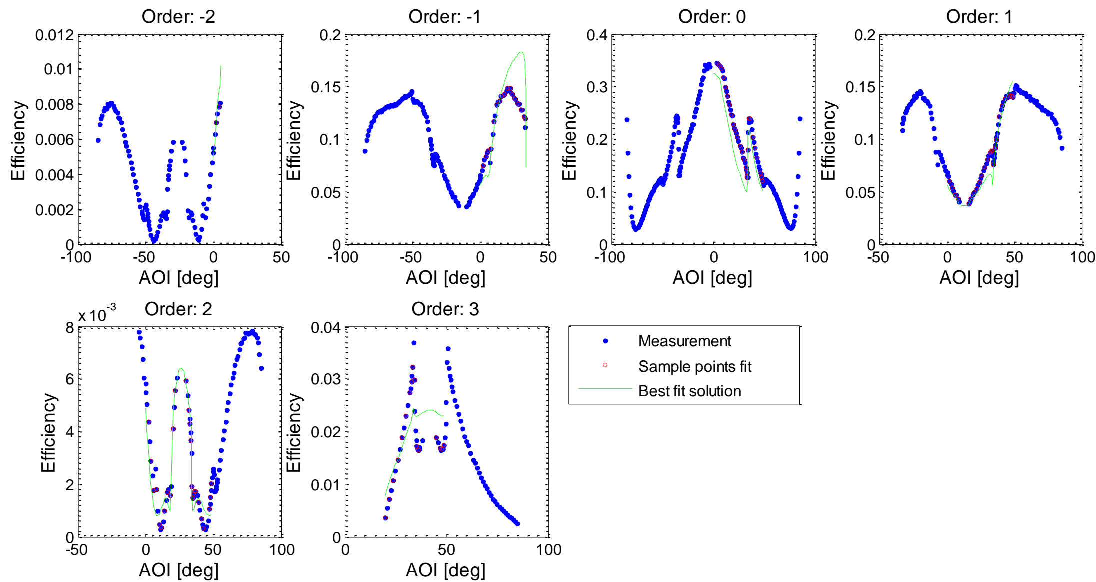

Figure 6 Diffraction efficiencies measured by DUV scatterometry together with the best fit solution based on the MLE evaluation. The sample points used for the reconstruction are marked red. Only one exemplary data set for p-polarized illumination at position 1 is shown.

The reconstructed structure parameters for each scatterometric system are listed in table 2. The stated "uncertainty" values are simply the uncertainty estimations resulting from the different nonlinear optimisation routines. They are by far no complete uncertainty estimations, since a lot of possible uncertainty contributions such as uncertainty estimations of parameters fixed in the optimisation process (such as the n&k-values of the silicon substrate), the limitations of the applied simplified structure models as well as possible limitations or errors of the measurement systems are still omitted. Realistic uncertainty values are expected to be about an order of magnitude larger.

Comparing the Fourier scatterometry results and least squares results of the goniometric scatterometry measurements in particular the CD, height and oxide layer thickness values are in reasonable agreement. The results obtained with the MLE method are in reasonable agreement with the least square results only for side wall angle and oxide layer thickness, however, for the CD and height values a severe mismatch is obtained.

Reconstruction parameter	DUV scatterometer		Fourier scatterometer
	MLE	Nonlinear least squares	Nonlinear least squares
Middle CD [nm]	301.5±1.5	277.5±1.2	277.0
Height [nm]	361.0±1.0	370.8±0.5	365.0
Side wall angle [°]	83.8±0.3	81.9±0.2	90.0
Oxide layer thickness [nm]	4.9±0.5	2.77±0.28	5.0
Bias value [nm]	-		150

Table 2 Best fit solution for the reconstruction parameters obtained by the goniometric DUV scatterometer and the Fourier scatterometer. The "uncertainties" given for the DUV scatterometer are directly given by the MLE method or estimated by the covariance matrix obtained from the least squares fit and are most likely drastically underestimated.

Downloaded From: http://www.spiedl.org/ on 01/16/2015 Terms of Use: http://spiedl.org/terms

5. DISCUSSION

We have presented a measurement comparison between two different scatterometric inspection methods: a goniometric DUV scatterometer and a coherent scanning Fourier scatterometer. They differ significantly from each other in the way how the sample is illuminated, how the diffraction efficiencies are detected and what information from the far field is used. The goniometric scatterometer illuminates the grating samples with only one distinct angle of incidence at one time and only records in plane diffraction efficiencies, which are typically well separated from each other. The Fourier scatterometer on the other hand illuminates the grating sample in parallel with all angles of incidence as provided by the microscope objective NA and detects all diffraction efficiencies, in plane as well as conical, at once and utilizes additional information provided by the coherent superposition of two diffraction orders in the Fourier plane of the setup. Effectively, with that also part of the phase information of the optical far field is accessible, but the information for different illumination and detection angles is somewhat merged and it might be complex to deconvolute these information.

The measurement on an etched 1D line grating with 600 nm pitch has shown that both systems are sensitive to the geometric parameters of the grating. The reconstructed CD and height values coincide within a few nanometers whereas the side wall angles are quite different. For side wall angles the Fourier scatterometry setup seems to have a reduced sensitivity as compared with the goniometric measurements, since only relatively low angles of incidences and the low zeroth and first diffraction orders are useable for the analysis, which might explain the observed slightly larger mismatch in terms of the sidewall angle. Furthermore, the side wall angle accuracy may be deteriorated by the large height/width aspect ratio of the lines.

The agreement for the results of the oxide layer thickness is reasonable, but not perfect. This is very likely due to the fact, that the evaluation of spectroscopic ellipsometry measurements as well as goniometric reflection measurements indicated, that this "oxide" layer is neither pure thermal nor native silicon oxide, but must include other unknown ingredients, too, maybe from the etching process. The approximation of this surface layer by an effective oxide layer can impact the reconstruction result particularly in view of the fact that both systems work at different wavelength ranges. Further characterizations of the surface layer with AFM and element specific methods like XPS would be necessary to fully characterize this layer [20]. This layer is assumed to be the reason, why there are slight differences of the results presented here as compared with the results given for model 1 as described in [10].

The comparison of two different evaluation techniques for the parameter reconstruction of the DUV scatterometry data reveals major deviations for the parameters CD and structure height. As mentioned above, the current MLE analysis is still preliminary, since not all available measurement data has been included, yet. However, the main reason for the obtained deviations can be probably attributed to the fact, that the MLE evaluation includes an estimation of the line roughness (LR, line edge roughness as well as line widths roughness). This evaluation indicates a line roughness of the order of 10 nm, which is in good quantitative agreement with first results of a currently performed SEM based evaluation of these grating structures.

Additionally former analysis have given a clear indication that the investigated silicon line structures have a significant amount of bottom corner rounding (footing). The influence of this footing, which for efficiency reasons has been neglected in this investigation, on the two different measurement methods and on the different data evaluation methods is not known and has to be further investigated carefully.

Finally, other reasons for different best fit parameter values may lie in neglecting an oxide layer at the side wall of the structure within the applied RCWA simulations. At the structure edges there will be very likely at least a thin native oxide layer, and it is still to be evaluated, if this is the case, how thick the sidewall oxide layer is and how this effects the different scatterometric measurement results. Further inspections are pending and measurements with other approved high resolution imaging inspection methods like AFM and SEM have been started or are planned. These results will support the analysis and will help to identify and reduce possible parameter correlations in data analysis of the scatterometric measurement data.

The partly mismatch of the results also demonstrates the necessity for a reliable reference standard especially with respect to traceability [21].

Downloaded From: http://www.spiedl.org/ on 01/16/2015 Terms of Use: http://spiedl.org/terms

Acknowledgments

The European Metrology Research Program (EMRP) is jointly funded by the EMRP participating countries within EURAMET and the European Union. We thank the European commission and the EURAMET e.v. for financial support under the support code no 912/2009/EC.

REFERENCES

1. M. Henn, H. Gross, F. Scholze, M. Wurm, C. Elster, and M. Bär, "A maximum likelihood approach to the inverse problem of scatterometry", Opt. Exp. 20, 12771-12786 (2012).
2. P. Boher, M. Luet, T. Leroux, J. Petit, P. Barritault, J. Hazart, P. Chaton, “Innovative Rapid Photo-goniometry method for CD metrology”, Proc. SPIE 5375 (2004) 1302.
3. P. Boher, J. Petit, T. Leroux, J. Foucher, Y. Desières, J. Hazart, P. Chaton, “Optical Fourier transform scatterometry for LER and LWR metrology”, Proc. SPIE 5752 (2005) 192.
4. N. Kumar ; O. El Gawhary ; S. Roy ; V. G. Kutchoukov ; S. F. Pereira, et al., “Coherent Fourier scatterometry: tool for improved sensitivity in semiconductor metrology”, Proc. SPIE 8324, Metrology, Inspection, and Process Control for Microlithography XXVI (2012)
5. V. F. Paz, et al. "Solving the inverse grating problem by white light interference Fourier scatterometry" Light: Science & Applications 1.11 e36 (2012)
6. C.J. Raymond, "Overview over scatterometry applications in high volume silicon manufacturing", AIP Conference Proceedings 788 (2005) 394-402
7. O. El Gawhary, N. Kumar, S.F. Pereira, W.M.J. Coene, H.P. Urbach, “Performance analysis of coherent optical scatterometry”, Appl. Phys. B 105 (2011) 775.
8. S. Roy, O. El Gawhary, N. Kumar, S. F. Pereira, H. P. Urbach, “Scanning effects in coherent Fourier scatterometry”, JEOS – Rapid Publications 7 (2012) 12031.
9. M. Wurm, S. Bonifer, B. Bodermann, J. Richter, “Deep ultraviolet scatterometer for dimensional characterization of nanostructures: system improvements and test measurements”, Meas. Sci. Technol. 22 (2011)
10. J. Endres, A. Diener, B. Bodermann, M. Wurm; “Investigations of the influence of common approximations in scatterometry for dimensional nanometrology”, Meas. Sci. Technol 25 (2014)
11. S. Roy, N. Kumar, S. F. Pereira and H. P. Urbach, “Interferometric coherent Fourier scatterometry: a method for obtaining high sensitivity in the optical inverse-grating problem”, J. Opt. 15 (2013) 2.
12. P. Petrik, N. Kumar, G. Juhasz, B. Fodor, S. F. Pereira, M. Fried, H. P. Urbach, “Fourier ellipsometry – an ellipsometric approach to Fourier scatterometry”, 8th Workshop Ellipsometry, 10-12 March, 2014, Dresden, Germany, to be published.
13. S. Roy, N. Kumar, S. F. Pereira and H. P. Urbach, “Interferometric coherent Fourier scatterometry: a method for obtaining high sensitivity in the optical inverse-grating problem”, J. Opt. 15 (2013) 075707
14. M. G. M. M. van Kraaij, “Forward diffraction modelling: Analysis and application to grating reconstruction”, PhD Thesis, Technical University of Eindhoven (http://alexandria.tue.nl/extra2/702579.pdf).
15. J. Elschner, R. Hinder, A. Rathsfeld, and G. Schmidt, http://www.wias-berlin.de/software/DIPOG
16. M.-A. Henn; H. Gross; S. Heidenreich; F. Scholze; C. Elster, and M. Bär, “Improved reconstruction of critical dimensions in extreme ultraviolet scatterometry by modeling systematic errors“, Meas. Sci. Technol. 25, 044003 (2014).
17. M.-A. Henn; H. Gross; S. Heidenreich; A. Rathsfeld and M. Bär, “Modelling of line roughness and its impact on the diffraction intensities and the reconstructed critical dimensions in scatterometry“, Appl. Opt. 51, 7384 (2012).
18. M.-A. Henn; H. Gross; S. Heidenreich; A. Rathsfeld and M. Bär, “Improved grating reconstruction by determination of line roughnedd in extreme ultraviolet scatterometry“, Opt. Lett, 37, 5229 (2012).
19. M.-A. Henn; S. Heidenreich; H. Gross; B. Bodermann, and M. Bär, ”The effect of line roughness on DUV scatterometry“, Proc. SPIE 8789 (2013).
20. N. Kumar, P. Petrik, S. F. Pereira, H. P. Urbach, “ Ellipsometric evaluation of unintentional surface layers and its influence on grating reconstruction in coherent Fourier scatterometry”, 8th Workshop Ellipsometry, 10-12 March, 2014, Dresden, Germany
21. B. Bodermann; P. E. Hansen; S. Burger ; M.-A. Henn ; H. Gross ; M. Bär ; F. Scholze ; J. Endres ; M. Wurm; ”First steps towards a scatterometry reference standard”, Proc. SPIE 8466, (2012), 84660E-1 - 84660E-12

Downloaded From: http://www.spiedl.org/ on 01/16/2015 Terms of Use: http://spiedl.org/terms